Inverse problems arising in different synthetic aperture radar imaging systems and a general Bayesian approach for them [*]

Sha Zhu[a,b], Ali Mohammad-Djafari[a], Xiang Li[b] and Junjie Mao[c]

[a]Laboratoire des Signaux et Systèmes, UMR8506 CNRS-SUPELEC-Univ.Paris-Sud XI, Supélec, Plateau de Moulon, 3 rue Juliot-Curie, 91192 Gif-sur-Yvette, France;
[b]Research Institute of Space Information Technology, School of Electronic Science and Engineering, National University of Defense Technology, Changsha 410073, Hunan, P.R.China;
[c]Research Center of Microwave Technology, School of Electronic Science and Engineering, National University of Defense Technology, Changsha 410073, Hunan, P.R.China

ABSTRACT

Synthetic Aperture Radar (SAR) imaging systems are nowadays very common technics of imaging in remote sensing and environment survey. There are different acquisition modes: spotlight, stripmap, scan; different geometries: mono-, bi- and multi-static; and varieties of specific applications: interferometric SAR (InSAR), polarimetric SAR etc. In this paper, first a common inverse problem framework for all of them is given, and then basics of SAR imaging and the classical deterministic inversion methods are presented. Aiming at overcoming the inadequacies of deterministic methods, a general probabilistic Bayesian estimation method is pioneered for solving image reconstruction problems. In particular, two priors which simply allow the automated determination of the hyperparameters in a *Type-II* likelihood framework are considered. Finally, the performances of the proposed methods on synthetic data.

Keywords: Inverse problem, Synthetic Aperture Radar, Bayesian inference, sparse reconstruction, hyperparameter estimation

1. INTRODUCTION

Inverse problem arises in many applications of Synthetic Aperture Radar (SAR) imaging systems.[1] The main explanation is that, like other imaging systems such as tomography, we are faced with the problem of determining the spatial distribution of an unknown object (scene) from direct measurements that are called an image (in tomography, which is from indirect measurements, called a projection).[2] An inverse problem in specific seeks to estimate an object from a forward model and observed data. Unlike the forward model that is well posed as defined by Hadammard: a problem is mathematically well posed if the solution of the problem satisfies three conditions: existence, uniqueness and stability,[3] with a finite number of discrete data items, a solution exists, but not unique; also, with the imperfect of the measurement device (modeling, linearizing and other unknown errors), called noise, the solution couldn't be stable.[4] The inverse problem for SAR imaging is always ill-posed.

To begin with our discussion, a very general form for the forward problem can be presented as follows:

$$g(\boldsymbol{s}) = [\mathcal{H}f(\boldsymbol{r})](\boldsymbol{s}) + \epsilon(\boldsymbol{r}), \quad \boldsymbol{r} \in \mathcal{R}, \boldsymbol{s} \in \mathcal{S} \tag{1}$$

where $\boldsymbol{g}$ denotes the observed data, $f(\boldsymbol{r})$ denotes the unknown objects(scene), $\boldsymbol{r}$ and $\boldsymbol{s}$ denotes the position, $\mathcal{R}$ and $\mathcal{S}$ denote whole original and observed image space respectively, $\mathcal{H}$ is an operator denoting the forward model, or to say, radar system response function, and ϵ denotes the noise.

*The Ph.D candidate is under a joint-supervision of UPS and NUDT, sponsored by China Scholarship Council(CSC)

Further author information: (Send correspondence to Sha Zhu)
Sha Zhu: E-mail: sha.zhu@lss.supelec.fr, Telephone: +33 (0)1 69 85 17 43
Ali Mohammad-Djafari: E-mail: djafari@lss.supelec.fr, Telephone: +33 (0)1 69 85 17 41

If the model is linear, which is a reasonable assumption for most cases of SAR imaging, the equation 1 can be written as:

$$\boldsymbol{g}(\boldsymbol{s}) = \int \boldsymbol{f}(\boldsymbol{r})\boldsymbol{h}(\boldsymbol{r},\boldsymbol{s})\ \mathrm{d}\boldsymbol{r} + \epsilon(\boldsymbol{s}). \tag{2}$$

If $\boldsymbol{h}(\boldsymbol{r},\boldsymbol{s}) = \boldsymbol{h}(\boldsymbol{r}-\boldsymbol{s})$, the relation becomes a convolution. When the data is discrete, $g(s)$ is a vector of M in a Euclidian space,

$$\boldsymbol{g}(\boldsymbol{s}_i) = \int \boldsymbol{h}(\boldsymbol{s}_i,\boldsymbol{r})\boldsymbol{f}(\boldsymbol{r})\ \mathrm{d}\boldsymbol{r} + \epsilon(\boldsymbol{s}_i), \quad i = 1,...,M \tag{3}$$

and we can write it in a vector-matrix form:

$$\boldsymbol{g} = \boldsymbol{H}\boldsymbol{f} + \boldsymbol{\epsilon} \tag{4}$$

where $\boldsymbol{g} = \{g(s), s \in \mathcal{S}\}$, $\boldsymbol{f} = \{f(r), r \in \mathcal{R}\}$ and $\boldsymbol{\epsilon} = \{\epsilon(r), r \in \mathcal{R}\}$ are vectors of the observed image, the unknown original object and observation errors, and $\boldsymbol{H}$ is a huge dimensional matrix.

In the case of a Multi Input and Multi Output (MIMO) system

$$\boldsymbol{g}_k(\boldsymbol{s}_i) = \sum_{l=1}^{L} \boldsymbol{H}_{kl}\boldsymbol{f}_l(\boldsymbol{r}) + \epsilon_k(\boldsymbol{s}_i), \quad k = 1,...,K \tag{5}$$

where we assumed K outputs and L inputs.

Until now, we clearly see that a general inverse problem is that given the forward model $\boldsymbol{H}$ and the data $\boldsymbol{g} = \{\boldsymbol{g}(\boldsymbol{s}_i), i = 1,...,M\}$ to estimate $\boldsymbol{f}(\boldsymbol{r})$. As it is ill posed we need to introduce prior information built from probabilistic methods.

Mathematically speaking, in a 2D case, the problem of SAR imaging, after some simplification,[5] as we will see in the next section in more details, becomes the Fourier Synthesis (FS) which consists of estimating an unknown function $f(x,y)$ (scene) from the partial and truncated information of its Fourier Transform (FT) $F(u,v)$. To focus our discussion on a general inversion method we present the relation between the FT of the observed signals and the 2D spatial FT of the scene by the following:

$$G(k_x,k_y) = M(k_x,k_y)F(k_x,k_y) \tag{6}$$

where

$$F(k_x,k_y) = \int f(x,y)\exp -j(k_x x + k_y y)\ \mathrm{d}x\ \mathrm{d}y. \tag{7}$$

where $k = \sqrt{k_x^2 + k_y^2} = 2\pi/f$ is the wave number, in the wavenumber domain, $F(k_x,k_y)$ is the FT of $f(x,y)$, $G(k_x,k_y)$ is the FT the observed data, and $M(k_x,k_y)$ is a binary valued function which is equal to one on the points where we have the data and zero elsewhere. In fact $M(k_x,k_y)$ is related to the radar frequency and measurement system geometries.

So the objective becomes image reconstruction of an inverse Fourier Synthesis (FS) problem,[6] i.e., to obtain $f(x,y)$ from $G(k_x,k_y)$. For simplest cases as mono-static where the radar transmitter and receiver are located in the same place, or bi-static, where the radar transmitter and receiver are located differently,[7,8] the objective is to find an optimal reconstruction; while for more complicated cases as multi-static, where the radar system has two or more transmitter or receiver antennas and all the distances between antennas are larger than their proper dimensions, specifically, the objective becomes data fusion for obtaining super-resolution images.

There are many inversion methods for inverse problems,[4,9–14] such as analytical methods (mathematical physics), parametric methods as least square and generalized inversion, and regularization methods. To solve FS problems in SAR imaging, one simple classic method is using the inverse Fourier Transform(IFT),[15,16] which is given as:

$$\widehat{f}(x,y) = IFT\{G(k_x,k_y)M(k_x,k_y)\} \tag{8}$$

the equation above turns to be a simple way

$$\widehat{f}(x,y) = IFT\{G(k_x,k_y)\} \tag{9}$$

on condition that we could obtain $M(k_x,k_y) = 1$ in the full wavenumber domain. The classical IFT methods assume all the unobserved dat (the values of $G(k_x,k_y)$ on those points where $M(k_x,k_y) = 0$) to be zero. Evidently, this is not the real case.

Besides the classic analytical method,[17] regularization theory has been playing a very important role for solving inverse problems in SAR imaging.[12] The regularization method is based on the prior information of the unknown object, trying to "restore" original information as much as possible. From this sense, the regularization method is proper to improve SAR imaging resolution. However, regularization methods have constraints: errors considered implicitly white and Gaussian, limited prior information on the solution, and lack of tools for the determination of the hyperparameters.

All of these inversion methods could be considered as "deterministic" methods. When considering radar imaging as an inverse problem, the main challenge for improving the resolution of generated SAR images, are:

i) In a classical view, if the radar frequency is given, its resolution is consequently defined. We need to develop data processing methods to improve its resolution.

ii) For a multi-static case, which is paid more and more attention to for the importance of cooperation surveillance for passive radars and in remote sensing filed for space distribution of satellite-borne SAR ,[1, 18, 19] the problem becomes making full use of multi-static and multi-frequency SAR data to achieve a higher resolution, which is called super-resolution.[20] Reference [21, 22] gave a review of recent developed fusion methods, indicating that a statistically based fusion method, relying on statical approaches which can estimate the pixel value relationship between all the input bands, can eliminate the problems of data set dependency which arises with classical fusion methods.

By employing the Bayesian inversion method, these problems can find their answers.[2] Concretely, this paper will be organized as follows:

Firstly, before talking about further details of inversion methods, to be more adapted to real cases, basics in different working modes of SAR and radar systems with three geometries are presented.

Then, in contrast of classical deterministic inversion methods, a Bayesian estimation approach for general inverse problems is investigated; for linear cases, the inverse FS problem has been well examined. We start with a general separable Gaussian prior case appropriate for the scenes with point sources and then extend it to more complex priors as Gaussian Markovian (GM) for representing the scene with the combination of different objects. Typically, two priors which simply allow the automated determination of the hyperparameters in a *Type-II* likelihood framework are considered.

Finally, we implemented the proposed method for simple reconstruction problems for mono- or bi-static SAR, as well as, the inversion and fusion method for multi-static SAR and compared the obtained results to those using the classical inversion methods.

2. SYNTHETIC APERTURE RADAR IMAGING

2.1 Varieties of SAR Imaging Systems

With the first radar appeared for military requirements during 1950s, throughout more than 60 years development, especially with the great rise in digital signal processing technology and its application in radar system design (particularly in data processing) in the last 30 years,[23] nowadays SAR is becoming a very common technics for high resolution imaging in application with varieties of systems: spotlight, stripmap, scan and different geometries: mono-, bi- and multi-static, which play an important role in remote sensing and environment survey.

2.1.1 Definition of "Resolution"

For researchers in radar signal processing or image processing field, the aim is to obtain a high resolution image which is helpful for later procedures as feature extraction or object classification.[24] In our text "Resolution" is defined as the minimum distance between two objects could be separated (for observation) in an image. High resolution acquired by SAR imaging is in both range and azimuth (cross-range) direction. The first is gained by pulse compression, and the latter is obtained by synthesis antenna. As its name indicated, synthetic aperture is a definition relative to "real aperture" of a radar antenna, which is a technique to synthesize a large antenna width achieved by utilizing the relative movement of the radar and observed scene then coherently integrating the returned signal pulse-to-pulse as the radar moves along its path. SAR makes use of the radar principle to form an high resolution image by its wide synthetic aperture.

However, for a real SAR system, since the hardware limitation as the antenna aperture and the power of the radar transmitter can't be elevated significantly, developing new data processing methods to improve SAR imaging resolution turns to be a very important way.[24] Classical supersolution imaging methods mainly are: extrapolation in frequency domain, iteration in space domain, spectrum estimation and regularization methods.[25,26] Recently Bayesian methods for SAR superresolution imaging are also presented.[20,27]

2.1.2 Different working modes of SAR: Stripmap, Spotlight and Scan SAR

SAR mainly works on two modes, spotlight and stripmap.[28] As shown in Figure 1, SpotSAR is by controlling the direction of antenna to obtain a high resolution SAR image of an interested object (or scene). Comparing to a fixed antenna, it has a long illuminate time towards the object (or scene).[29] In strip SAR, the squint angle between the beam direction and the flight path (assuming as a line) keeps a fixed angle, and a stripmap on the ground which is parallel to the flight path can be observed continuously. StripSAR is mainly used for large area imaging, which doesn't require a very high resolution. Besides these two modes mentioned above, there also exists a scan SAR where the strip on the ground is not parallel to the flight path, so the SNR(signal to noise ratio) will be decreased as range increases. In this paper, we mainly consider the spot SAR which can get a high resolution.

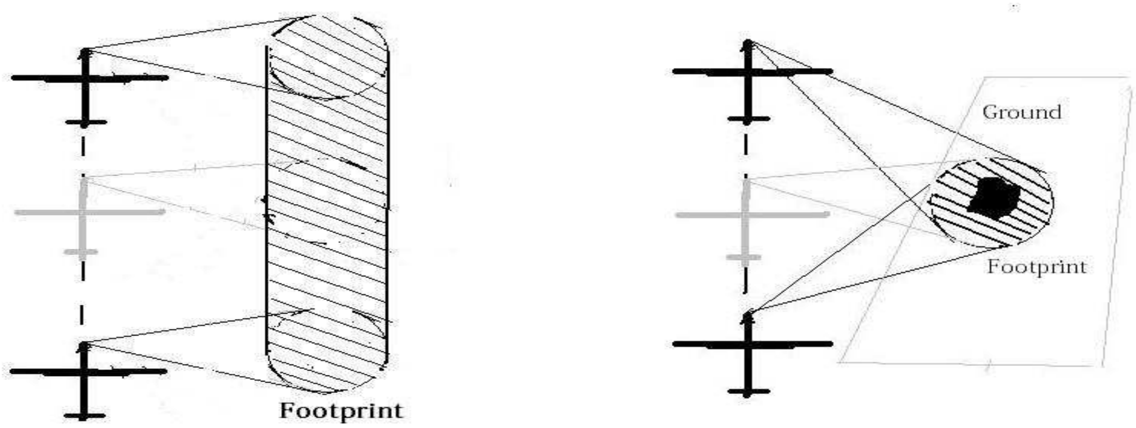

Strip SAR　　　　Spot SAR

Figure 1. Strip and Spot SAR

2.1.3 Different geometries of SAR: mono-, bi- and multi-static SAR

According to equation 1, for $M = N = 1$, that is one set of data, which are received from the transmitter at the same location (mono-static) or received by another receiver antenna at a different position (bi-static); for $M > 2$ and $N = 1$, that is two or more data sets in multi-static cases. Geometries are shown in Figure 2.

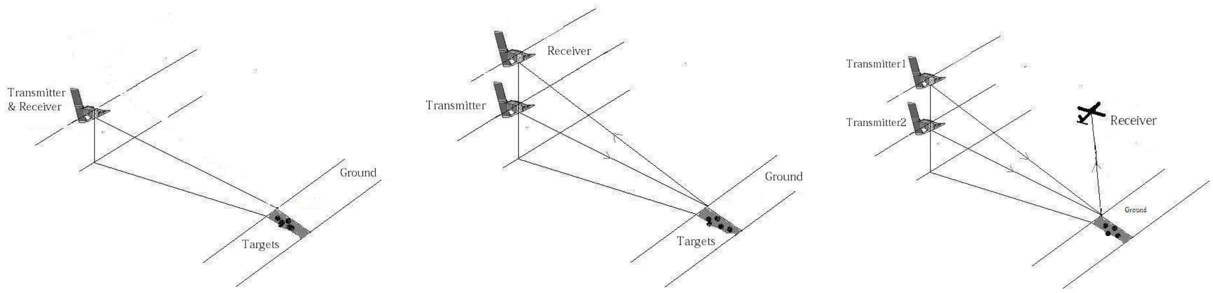

monostatic bistatic multistatic

Figure 2. Geometries

2.2 Forward Modeling: Radar Scattering

In 2D case, with some simplifications of the forward model, the relation between the emitted signal $p(t)$ and the received signal $s(t)$ reflected from a point source $f(m,n)$ located at the position (x_m, y_n) can be written as $s(t) = f(m,n)p(t-\tau_{m,n})$ where $\tau_{m,n}$ represent the delay time between the emitted and received signal. When the position of this emitter-receiver changes along the axis u, as shown in Figure (3, the received signal at the position u can be written as

$$s(t,u) = \sum_m \sum_n f(m,n)\, p(t-\tau_{m,n}(u)). \tag{10}$$

This expression can be extended to the continuous case:

$$s(t,u) = \iint f(x,y)\, p(t-\tau(x,y,u))\ \mathrm{d}x\ \mathrm{d}y. \tag{11}$$

Now, if we parametrize the position of the emitter by the angle θ of the line joining it to the center of the scene and noting by

$$\boldsymbol{k} = \begin{bmatrix} k_x \\ k_y \end{bmatrix} = \begin{bmatrix} k\cos(\theta) \\ k\sin(\theta) \end{bmatrix}, \qquad |\boldsymbol{k}| = k = \omega/c \tag{12}$$

then, we can write

$$s(\omega,\theta(u)) = P(\omega) \iint f(x,y)\ \exp\left[-j\omega\tau(x,y,\theta(u))\right]\ \mathrm{d}x\ \mathrm{d}y \tag{13}$$

where

$$\tau(x,y,u(\theta)) = \frac{2}{c}\sqrt{x^2+(y-u)^2} = \frac{2}{\omega}(k_x x + k_y(y-u)) \tag{14}$$

Putting this expression into the previous equation, we get:

$$s(\omega,\theta(u)) = P(\omega) \iint f(x,y)\ \exp\left[-j(k_x x + k_y y)\right]\ \mathrm{d}x\ \mathrm{d}y \tag{15}$$

We can then recognize a FT equation between the spectrum of the received signal and the 2D FT of the scene and the two variables which are important: the angle θ and the bandwidth of the emitted signal. This relation is summarized on Figure 3.

In the bi-static and multi-static cases, we can also write in the same way:

$$s(t,u) = \iint f(x,y)\, p(t-\tau_{tc}(x,y)-\tau_{rc}(x,y,u(\theta)))\ \mathrm{d}x\ \mathrm{d}y \tag{16}$$

where, this time, as it is shown in Figure 4, we have:

$$\tau_{tc} + \tau_{cr} = \frac{2}{\omega}(k_x x + k_y(y-u)) \tag{17}$$

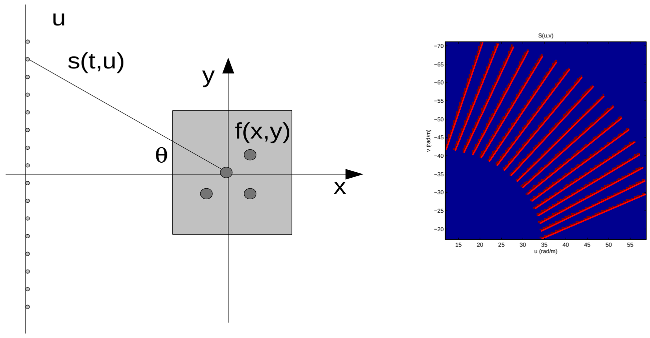

$$k_x = k\,\cos(\theta)$$

$$k_y = k\,\sin(\theta)$$

Figure 3. Mono-static SAR Imaging geometry and relations

and again following the same steps, by defining:

$$\boldsymbol{k} = \begin{bmatrix} k_x \\ k_y \end{bmatrix} = \begin{bmatrix} k\,(\cos(\theta_{tc}) + \cos(\theta_{cr}) \\ \\ k\,(\sin(\theta_{tc}) + \sin(\theta_{cr}) \end{bmatrix}, \qquad |\boldsymbol{k}| = k = \omega/c \tag{18}$$

we can deduce the same FT relation:

$$s(\omega, \theta_{tc}, \theta_{cr}) = P(\omega) \iint f(x, y)\, \exp\left[-j(k_x x + k_y y)\right]\, \mathrm{d}x\, \mathrm{d}y \tag{19}$$

but this time, the relations between (k_x, ky) and (u, θ) will be different, as it is shown on Figure 4.

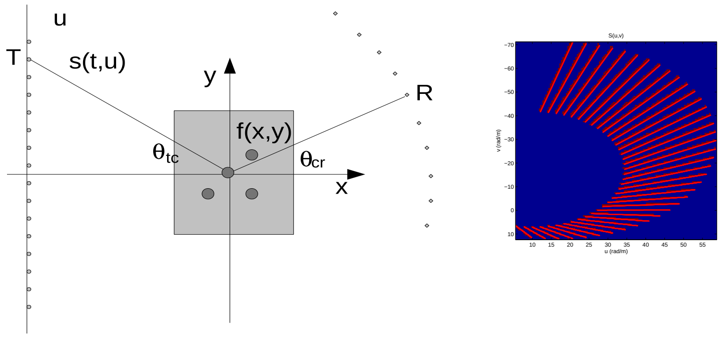

$$k_x = k\,(\cos(\theta_{tc}) + \cos(\theta_{cr})$$

$$k_y = k\,(\sin(\theta_{tc}) + \sin(\theta_{cr})$$

Figure 4. Bi-static and Multistatic SAR Imaging geometry and relations

In summary, in all three cases, the spectrum of each received signal $S(\omega, \theta)$ at a given angle θ in mono-static case, and $S(\omega, \theta_{tc}, \theta_{cr})$ at a given angles of transmitter-receiver $(\theta_{tc}, \theta_{cr})$ in the bi-static and multi-static cases, give some information in the Fourier domain $F(k_x, k_y)$ of the scene on a segment of a straight line whose length depends on the bandwidth of the emitted signal and its orientation on the geometry of the transmitter-receiver. Unfortunately, at one hand, due to the bandwidth limitation of the emitted signal $P(\omega)$ and limitation of the angles, the Fourier domain will not be complete. The inverse problem is then ill-posed. The classical methods of inversion, just do interpolation and zero-filling extrapolation and use the Inverse FT to propose a solution. As, we will see, in the following sections, we consider the problem as a Fourier Synthesis (FS) inverse problem.

The forward modeling and inversion for the three geometries are indicated as the following:

- mono-, or bi-static SAR

$$\begin{array}{c|c|c} f(x,y) & \longrightarrow F(k_x,k_y) \longrightarrow M(k_x,k_y), G(k_x,k_y) & \longrightarrow \boxed{\text{Reconstruction}} \longrightarrow \widehat{f}(x,y) \\ \text{Original target} & \text{Forward modeling} & \text{Inversion} \end{array}$$

  This model could be easily extended to a more complicated case: multi-static SAR.

- multi-static SAR

$$\begin{array}{c|c|c} f(x,y) & \longrightarrow F(k_x,k_y) \longrightarrow \begin{array}{c} M_1(k_x,k_y)\ G_1(k_x,k_y) \\ M_2(k_x,k_y)\ G_2(k_x,k_y) \end{array} & \longrightarrow \boxed{\begin{array}{c}\text{Data Fusion} \\ \text{and Reconstruction}\end{array}} \longrightarrow \widehat{f}(x,y) \\ \text{Original target} & \text{Forward modeling} & \text{Fusion and inversion} \end{array}$$

There are also some specific applications for SAR, such as the interferometric SAR (InSAR),[30] polarimetric SAR[31].[32] Limited by the length, they are not discussed here.

One of advanced SAR imaging techniques is focusing on the case of a small number of transmitters and receivers, i.e multi-static situation and handing sparse data.[1] In our work, we will emphasize on handling these two cases, with a jointly Bayesian fusion and reconstruction method and a sparse radar reconstruction method proposed respectively.

2.3 Classical inversion Methods and Constraints

There are several methods for solving inverse problems as analytical and regularization methods.

2.3.1 Analytical methods

In analytical methods (or to say mathematical physics), the inversion becomes

$$\widehat{\boldsymbol{f}}(\boldsymbol{r}) = \int \boldsymbol{w}(\boldsymbol{s},\boldsymbol{r})\boldsymbol{g}(\boldsymbol{s})\ \mathrm{d}\boldsymbol{s} \tag{20}$$

$\boldsymbol{w}(\boldsymbol{s},\boldsymbol{r})$ minimizing: $Q(\boldsymbol{w}(\boldsymbol{s},\boldsymbol{r})) = ||\boldsymbol{g}(\boldsymbol{s}) - [\boldsymbol{H}\widehat{\boldsymbol{f}}(\boldsymbol{r})](\boldsymbol{s})||_2^2$
Actually, Fourier Transform is just for this case.

$$\boldsymbol{g}(\boldsymbol{s}) = \int \widehat{\boldsymbol{f}}(\boldsymbol{r}) \exp\{-j\boldsymbol{s}.\boldsymbol{r}\} \tag{21}$$

$$\boldsymbol{h}(\boldsymbol{s},\boldsymbol{r}) = \exp\{-j\boldsymbol{s}.\boldsymbol{r}\} \ \text{ that means } \ \boldsymbol{w}(\boldsymbol{s},\boldsymbol{r}) = \exp\{+j\boldsymbol{s}.\boldsymbol{r}\} \tag{22}$$

so,

$$\widehat{\boldsymbol{f}}(\boldsymbol{r}) = \int \boldsymbol{g}(\boldsymbol{s}) \exp\{+j\boldsymbol{s}.\boldsymbol{r}\}\ \mathrm{d}\boldsymbol{s} \tag{23}$$

As we have discussed above, IFT can't be a satisfactory inversion method for SAR imaging.

2.3.2 Regularization methods

Regularization methods are aiming at finding a stable solution to an ill-posed inverse problem by minimizing of a compound criterion as:[13]

$$\widehat{\boldsymbol{f}} = \arg\min_{\boldsymbol{f}} \{J(\boldsymbol{f})\} \tag{24}$$

with

$$J(\boldsymbol{f}) = \triangle_1(\boldsymbol{g}, \boldsymbol{H}\boldsymbol{f}) + \lambda \triangle_2 (\boldsymbol{f}, \boldsymbol{f}_0) \tag{25}$$

where $\triangle_1$ and $\triangle_2$ are two distances, λ is the regularization parameter which regulates the compromise of the two terms and $\boldsymbol{f}_0$ is an *aprior* solution.

The main problems of regularization methods are: determination of the regularization parameter, the arguments of choosing two distances which are manually decided depending on personal experience, and quantification of the uncertainties associated with the obtained solutions. In the next section, we will see these inadequacies could be overcome by the Bayesian estimation framework.

3. BAYESIAN ESTIMATION FRAMEWORK

Recovering the scene $\boldsymbol{f}$ from non-complete observations $\boldsymbol{g}$ is generally ill-posed so that a certain prior knowledge has to be included to obtain an unique and stable solution. In this paper, we encode such prior knowledge using the Bayesian methodology in a coherent way. The likelihood probability $p(\boldsymbol{g}|\boldsymbol{f}, \boldsymbol{\theta}_1)$ is defined from the forward observation model $\boldsymbol{g} = \boldsymbol{H}\boldsymbol{f} + \boldsymbol{\epsilon}$ while the prior knowledge about the unknowns $\boldsymbol{f}$ is translated through the prior probability $p(\boldsymbol{f}|\boldsymbol{\theta}_2)$. Then the posterior probability of the unknowns $\boldsymbol{f}$ given by the observations $\boldsymbol{g}$ is expressed as

$$p(\boldsymbol{f}|\boldsymbol{g}, \boldsymbol{\theta}) = \frac{p(\boldsymbol{g}|\boldsymbol{f}, \boldsymbol{\theta}_1)\, p(\boldsymbol{f}|\boldsymbol{\theta}_2)}{p(\boldsymbol{g}|\boldsymbol{\theta})} \tag{26}$$

where $\boldsymbol{\theta} = (\boldsymbol{\theta}_1, \boldsymbol{\theta}_2)$ are the hyperparameters and

$$p(\boldsymbol{g}|\boldsymbol{\theta}) = \int p(\boldsymbol{g}|\boldsymbol{f}, \theta_1)\, p(\boldsymbol{f}|\theta_2)\; \mathrm{d}\boldsymbol{f} \tag{27}$$

is the so-called evidence of the model. Once we obtain this posterior probability of $\boldsymbol{f}$, the estimation of $\boldsymbol{f}$ can be either the *maximum a posterior* (MAP)

$$\widehat{\boldsymbol{f}} = \arg\max_{\boldsymbol{f}} p(\boldsymbol{f}|\boldsymbol{g}, \boldsymbol{\theta}) \tag{28}$$

or the Mean Square Error(MSE) estimator

$$\widehat{\boldsymbol{f}} = \int \boldsymbol{f}\, p(\boldsymbol{f}|\boldsymbol{g}, \boldsymbol{\theta})\; \mathrm{d}\boldsymbol{f}. \tag{29}$$

Unlike classic regularization estimation models, a fully Bayesian treatment of the estimation model allow us to adjust the hyperparmeters through maximizing the marginal likelihood, or evidence of model, or *Type-II* maximum likelihood.

$$\hat{\boldsymbol{\theta}} = \arg\max_{\boldsymbol{\theta}} p(\boldsymbol{g}|\boldsymbol{\theta}) \tag{30}$$

3.1 A Simple Gaussian Prior Model

We begin with considering a simple Gaussian Prior Model

$$p(\boldsymbol{f}|\sigma_f^2) = \mathcal{N}(\boldsymbol{f}|\mathbf{0}, \sigma_f^2\boldsymbol{I}) \tag{31}$$

which allows us easily computing the posterior probability $p(\boldsymbol{f}|\boldsymbol{g})$ and the evidence of model $p(\boldsymbol{g}|\boldsymbol{\theta})$. Combining with the Gaussian likelihood

$$p(\boldsymbol{g}|\boldsymbol{f}, {\sigma_\epsilon}^2) = \mathcal{N}(\boldsymbol{g}|\boldsymbol{H}\boldsymbol{f}, {\sigma_\epsilon}^2\boldsymbol{I}) \tag{32}$$

gives the posterior probability of f

$$p(\boldsymbol{f}|\boldsymbol{g}, {\sigma_\epsilon}^2, \sigma_f^2) = \mathcal{N}(\boldsymbol{f}|\boldsymbol{\mu}_f, \boldsymbol{\Sigma}_f) \tag{33}$$

with

$$\boldsymbol{\mu}_f = {\sigma_\epsilon}^{-2}\boldsymbol{\Sigma}_f \boldsymbol{H}^t \boldsymbol{g} \tag{34}$$

$$\boldsymbol{\Sigma}_f^{-1} = \sigma_f^{-2}\boldsymbol{I} + {\sigma_\epsilon}^{-2}\boldsymbol{H}^t\boldsymbol{H} \tag{35}$$

It is noteworthy that ${\sigma_\epsilon}^2/\sigma_f^2$ can be interpreted as the regularization parameter λ in the regularization model but with a big difference that a fully Bayesian treatment of the model is of capability of automatic determination of these parameters ${\sigma_\epsilon}^2, \sigma_f^2$. For this we can assign them Inverse Gamma priors and try to estimate them either jointly with $\boldsymbol{f}$ or first estimate them using the ML and then use them for inversion step.

The evidence of the model in such a simple case is

$$p(\boldsymbol{g}|{\sigma_\epsilon}^2, \sigma_f^2) = \left(\frac{1}{2\pi{\sigma_\epsilon}^2}\right)^{\frac{N}{2}} \left(\frac{1}{\sigma_f^2}\right)^{\frac{M}{2}} |\sigma_f^{-2}\boldsymbol{I} + {\sigma_\epsilon}^{-2}\boldsymbol{H}^t\boldsymbol{H}|^{-\frac{1}{2}} \exp\{-\frac{\|\boldsymbol{g} - \boldsymbol{H}\boldsymbol{\mu}_f\|^2}{2{\sigma_\epsilon}^2} - \frac{\|\boldsymbol{\mu}_f\|^2}{2\sigma_f^2}\} \tag{36}$$

Taking the logarithms of evidence of the model yields the log-marginal likelihood

$$\begin{aligned} \ln p(\boldsymbol{g}|{\sigma_\epsilon}^2, \sigma_f^2) = &-\frac{M}{2}\ln\sigma_f^2 - \frac{N}{2}\ln{\sigma_\epsilon}^2 \\ &- \frac{1}{2{\sigma_\epsilon}^2}\|\boldsymbol{g} - \boldsymbol{H}\boldsymbol{\mu}_f\|^2 - \frac{1}{2\sigma_f^2}\boldsymbol{\mu}_f^t\boldsymbol{\mu}_f - \frac{1}{2}\ln|\sigma_f^{-2}\boldsymbol{I} + {\sigma_\epsilon}^{-2}\boldsymbol{H}^t\boldsymbol{H}| - \frac{N}{2}\ln(2\pi) \end{aligned} \tag{37}$$

Denoted by γ_i the M greatest eigenvalues of the matrix ${\sigma_\epsilon}^{-2}\boldsymbol{H}^t\boldsymbol{H}$, the Equation (37) can be written as

$$\begin{aligned} \ln p(\boldsymbol{g}|{\sigma_\epsilon}^2, \sigma_f^2) = &-\frac{M}{2}\ln\sigma_f^2 - \frac{N}{2}\ln{\sigma_\epsilon}^2 \\ &- \frac{1}{2{\sigma_\epsilon}^2}\|\boldsymbol{g} - \boldsymbol{H}\boldsymbol{\mu}_f\|^2 - \frac{1}{2\sigma_f^2}\boldsymbol{\mu}_f^t\boldsymbol{\mu}_f - \frac{1}{2}\sum_{i=1}^{M}\ln(\sigma_f^{-2} + \gamma_i) - \frac{N}{2}\ln(2\pi) \end{aligned} \tag{38}$$

Setting the derivatives of the marginal likelihood with respect to ${\sigma_\epsilon}^2, \sigma_f^2$ to zeros gives

$${\sigma_\epsilon}^2 = \frac{\|\boldsymbol{g} - \boldsymbol{H}\boldsymbol{\mu}_f\|^2}{N - \gamma} \tag{39}$$

$$\sigma_f^2 = \frac{\boldsymbol{\mu}_f^t\boldsymbol{\mu}_f}{\gamma} \tag{40}$$

with $\gamma = \sum_{i=1}^{M}\frac{\gamma_i}{\gamma_i + \sigma_f^{-2}}$. Note the estimations of ${\sigma_\epsilon}^2, \sigma_f^2$ depend on the estimation of $\boldsymbol{f}$ which itself depends on ${\sigma_\epsilon}^2, \sigma_f^2$. Herein we adopted an iterative procedural that estimates $\boldsymbol{f}$ given by Equation 34 holding the ${\sigma_\epsilon}^2, \sigma_f^2$ fixed and then finds ${\sigma_\epsilon}^2, \sigma_f^2$ by fixing $\boldsymbol{\mu}_f$. This process is repeated until convergence.

3.2 Sparse Gaussian Prior

In this section we propose a sparse Gaussian prior as the one used usually in the Sparse Bayesian Learning (SBL) framework[33] that is

$$p(\boldsymbol{f}|\boldsymbol{\Sigma}^2) = \prod_{i=1}^{M}\mathcal{N}(f_i|0, \sigma_i^2) \tag{41}$$

with $\boldsymbol{\Sigma}^2 = (\sigma_1^2, \ldots, \sigma_M^2)$. Similar to the derivation of the simple case of Gaussian prior, the posterior probability of $\boldsymbol{f}$ is

$$p(\boldsymbol{f}|\boldsymbol{g}, {\sigma_\epsilon}^2, \boldsymbol{\Sigma}^2) = \mathcal{N}(\boldsymbol{f}|\boldsymbol{\mu}_f, \boldsymbol{\Sigma}_f) \tag{42}$$

with

$$\boldsymbol{\mu}_f = \sigma_\epsilon{}^{-2}\boldsymbol{\Sigma}_f \boldsymbol{H}^t \boldsymbol{g} \tag{43}$$

$$\boldsymbol{\Sigma}_f^{-1} = \boldsymbol{A} + \sigma_\epsilon{}^{-2}\boldsymbol{H}^t\boldsymbol{H} \tag{44}$$

with $\boldsymbol{A} = \mathrm{diag}(\sigma_1^{-2}, \ldots, \sigma_M^{-2})$. The evidence of the model is

$$p(\boldsymbol{g}|\sigma_\epsilon{}^2, \boldsymbol{\Sigma}_2) = (2\pi)^{-N/2}|\sigma_\epsilon{}^2 + \boldsymbol{H}\boldsymbol{A}^{-1}\boldsymbol{H}|^{-1/2} \exp\{-\frac{1}{2}\boldsymbol{g}^t(\sigma_\epsilon{}^2 + \boldsymbol{H}\boldsymbol{A}^{-1}\boldsymbol{H})^{-1}\boldsymbol{g}\} \tag{45}$$

Maximizing this evidence of the model gives the estimation of $\sigma_\epsilon{}^2$ and $\boldsymbol{\Sigma}_i^2$

$$\sigma_i^2 = \frac{\mu_i^2}{\gamma_i} \tag{46}$$

$$\sigma_\epsilon{}^2 = \frac{\|\boldsymbol{g} - \boldsymbol{H}\boldsymbol{\mu}_f\|^2}{N - \sum_i \gamma_i} \tag{47}$$

with $\gamma_i = 1 - \Sigma_{ii}^{-1}/\sigma_i^2$ where Σ_{ii}^{-1} is the diagonal element of the matrix $\boldsymbol{\Sigma}_{\boldsymbol{f}}{}_f^{-1}$.

3.3 Other Priors

The Bayesian framework permits us to conveniently extend the previous Gaussian prior model to more sophisticated models. We consider four prior models in this paper

1. Separable Generalized Gaussian (SGG)

$$p(\boldsymbol{f}) \propto \exp\{-\gamma \sum_j |f|_j^\beta\} \tag{48}$$

   with $1 \leq \beta \leq 2$. $\beta = 2$ is corresponding to the Gaussian model while $\beta = 1$ is the classic l_1 sparse model.

2. Separable Cauchy (SC)

$$p(\boldsymbol{f}) \propto \prod_j \frac{1}{\sqrt{1 + |f_j|^2}} \propto \exp\{-\frac{1}{2}\sum_j \ln(1 + |f_j|^2)\} \tag{49}$$

3. General Markovian priors

$$p(\boldsymbol{f}) \propto \exp\{-\gamma \sum_j \phi(f_j - f_{j-1})\} \tag{50}$$

   where $\phi(t)$ is the potential function which can be , for example, $t^2, |t|^\beta, \ln(1 - |t|^2)$

4. Generalized Gauss-Markov (GGM)

$$p(\boldsymbol{f}) \propto \exp\{-\gamma_1 \sum_j |f_j|^\beta - \gamma_2 \sum_j |f_j - f_{j-1}|^\beta\} \tag{51}$$

3.4 Multi-static data fusion model

Taking two data sets from multi-static SAR for an example, we can obtain two different observations $G_1(u, v), G_2(u, v)$ of the same target $f(x, y)$ from two sensors , respectively,

$$\begin{cases} \boldsymbol{g}_1 & = \boldsymbol{H}_1\boldsymbol{f} + \boldsymbol{\epsilon}_1 \\ \boldsymbol{g}_2 & = \boldsymbol{H}_2\boldsymbol{f} + \boldsymbol{\epsilon}_2 \end{cases} \tag{52}$$

Assuming the $\boldsymbol{\epsilon}_1, \boldsymbol{\epsilon}_2$ to be Gaussian and the prior $\boldsymbol{f}$ to be also Gaussian. Then the MAP estimation of $\boldsymbol{f}$ is

$$\widehat{\boldsymbol{f}} = \arg\max_{\boldsymbol{f}} p(\boldsymbol{f}|\boldsymbol{g}_1, \boldsymbol{g}_2, \boldsymbol{\theta}) = \arg\min_{\boldsymbol{f}} J(\boldsymbol{f}) \tag{53}$$

where

$$J(\boldsymbol{f}) = \frac{1}{\sigma_{\epsilon 1}^2}\|\boldsymbol{g}_1 - \boldsymbol{H}_1\boldsymbol{f}\|^2 + \frac{1}{\sigma_{\epsilon 2}^2}\|\boldsymbol{g}_1 - \boldsymbol{H}_2\boldsymbol{f}\|^2 + \frac{1}{\sigma_{\epsilon_f}^2}\|\boldsymbol{f}\|^2 \tag{54}$$

with the hyperparamters can be estimated approximately

$$\sigma_{\epsilon 1}^2 = \frac{\|\boldsymbol{g}_1 - H_1\widehat{\boldsymbol{f}}\|^2}{N_1}, \quad \sigma_{\epsilon 2}^2 = \frac{\|\boldsymbol{g}_2 - H_2\widehat{\boldsymbol{f}}\|^2}{N_2}, \quad \sigma_{\epsilon_f}^2 = \frac{\|\widehat{\boldsymbol{f}}\|^2}{M} \tag{55}$$

4. RESULTS WITH SIMULATED DATA

4.1 Synthetic data for mono and bi static cases

In this section we conduct experiments on synthetic data to validate our proposed method. Two synthetic data are generated, as shown in the Figure 5, first creating two original targets $f(x, y)$ and its Fourier transform $F(u, v)$ in wavenumber domain, then defining two binary valued masks $M(u, v)$ in the wavenumber domain for each target representing the geometry of the two different measurement strategies and finally the observations $G(u, v)$ are generated by $G(u, v) = F(u, v)M(u, v)$ and their corresponding signal in spatial domain $g(x, y)$ which is the inverse Fourier transform of $G(u, v)$. Our goal is to reconstruct the original scene $\hat{f}(x, y)$ from the partial observations $g(x, y)$.

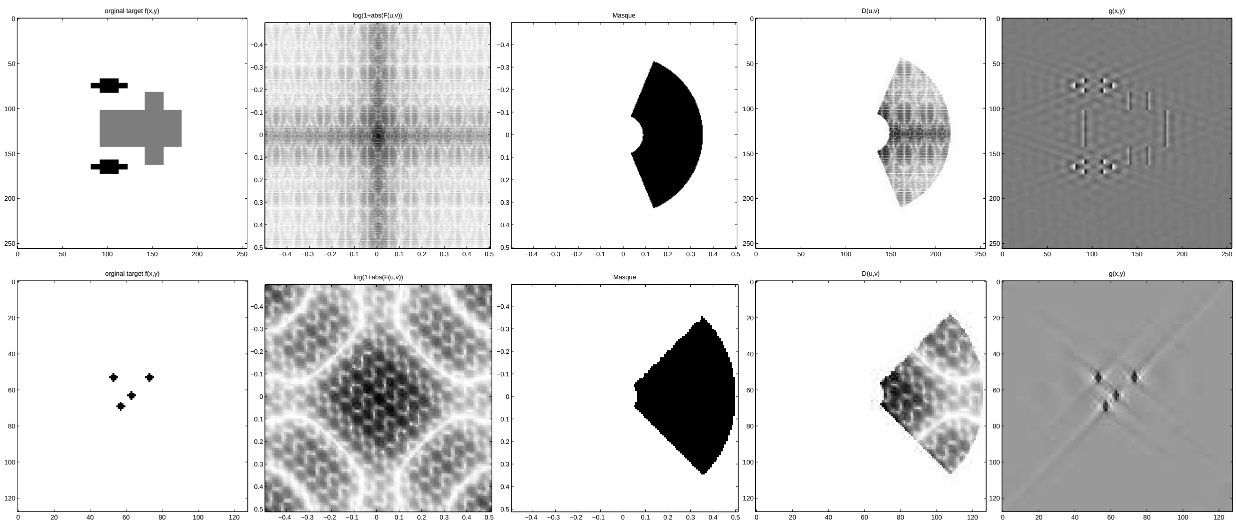

Original $f(x, y)$ F(u,v) Masque $M(u, v)$ G(u,v) $g(x, y)$

Figure 5. The two generated data.

Figure 6 shows the reconstructed results $\hat{f}(x, y)$ obtained through classic inverse fourier transform (IFFT) as well as different regularization models. In Figure 7, the MAP estimation with different priors are shown.

4.2 Simulating multi static data and results of Fusion and Inversion

In the first experiment, we use only one dataset (represents one band) to do reconstruction and then, we use both data sets to do joint data fusion and inversion by simulating data on real cases. There are target compositions by 4 spheres, and two sets of data corresponding to two bandwidth, simulating by different Masques $M_1(u, v)$ and $M_2(u, v)$. Figure 8 shows the fusion results.

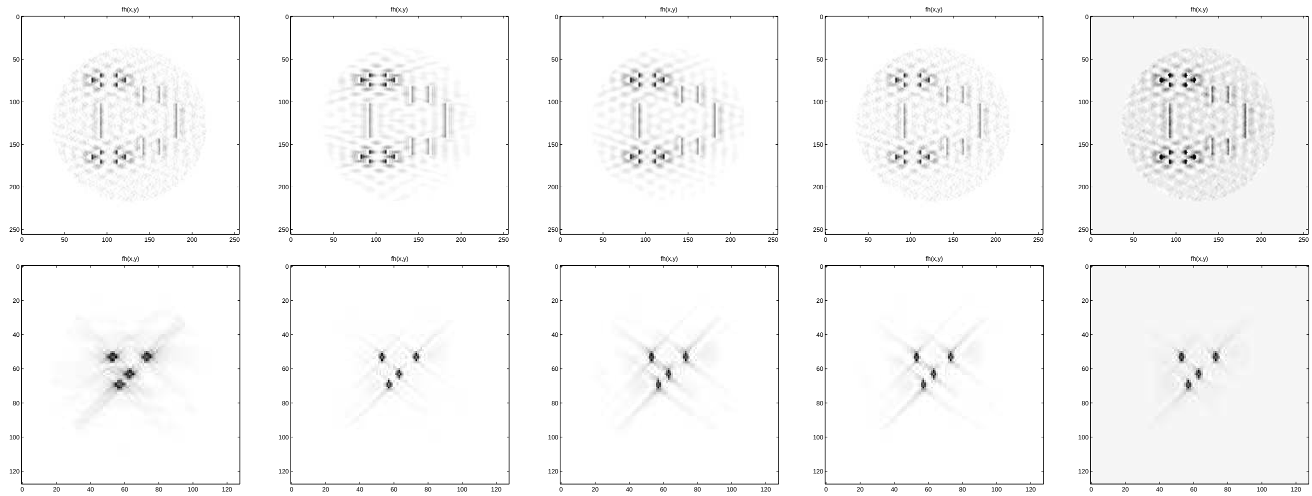

IFFT | Gerchberg-Papuoulis | Least Square | Quadratic Regul. | L2L1 regularization

Figure 6. Reconstructed Results from IFFT and different regularization model.

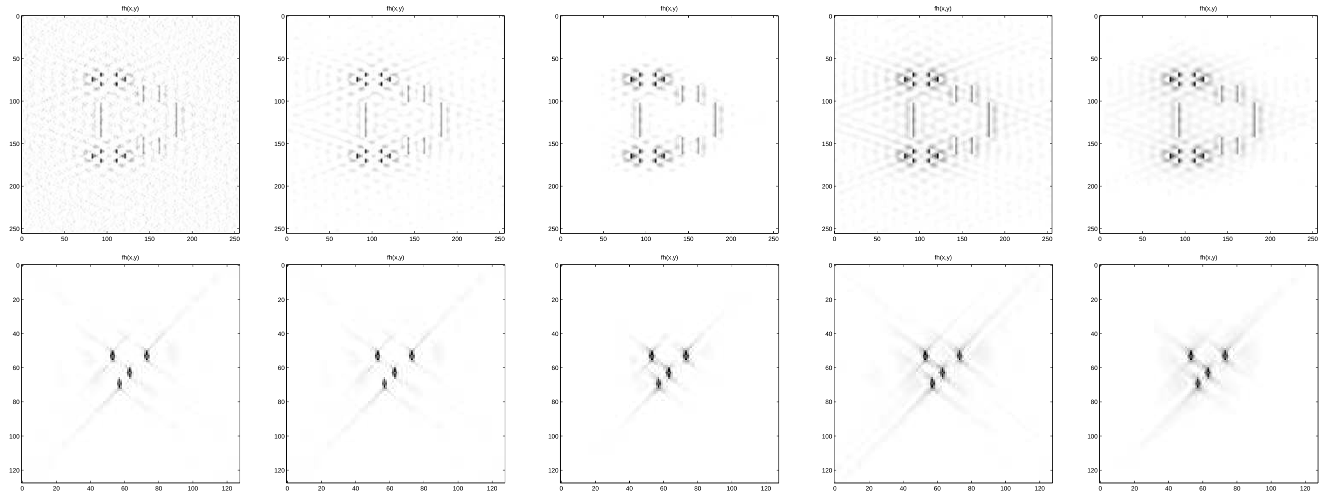

Gaussian | Sparse Gaussian | Generalized Gaussian | Cauchy | Gen. Gauss-Markov

Figure 7. Bayesian reconstruction with different priors: a) Gaussian prior with hyperparameter estimation, b) Sparse Gaussian prior with hyperparameter estimation, c) Generalized Gaussian , d) Cauchy, d) Generalized Gauss-Markov

5. CONCLUSIONS AND PERSPECTIVES

In this paper, we cast the ill-posed inverse problems on different SAR imaging systems in a general Bayesian framework, which can conveniently translate our knowledge about the target to regularize the estimation. The appropriate prior model can lead to a stable and coherent reconstruction of the original targets from the partial observations. In particular, we consider two simple Gaussian priors which allow easily estimating the hyperparameters simultaneously in a Type-II maximum likelihood framework. The results obtained by the proposed method on simulated data has shown a good performance.

SAR imaging is a very complicated electromagnetic scattering inverse problem. Future work could be conducted in three aspects: i) Establishing proper radar scattering models. ii) Investigating methods to estimate the hyperparameters for more complicated priors for real cases, e.g., variational approximate method or Monte carlo approximate method. iii) Proposing new data fusion methods for SAR super-resolution (SR) imaging.

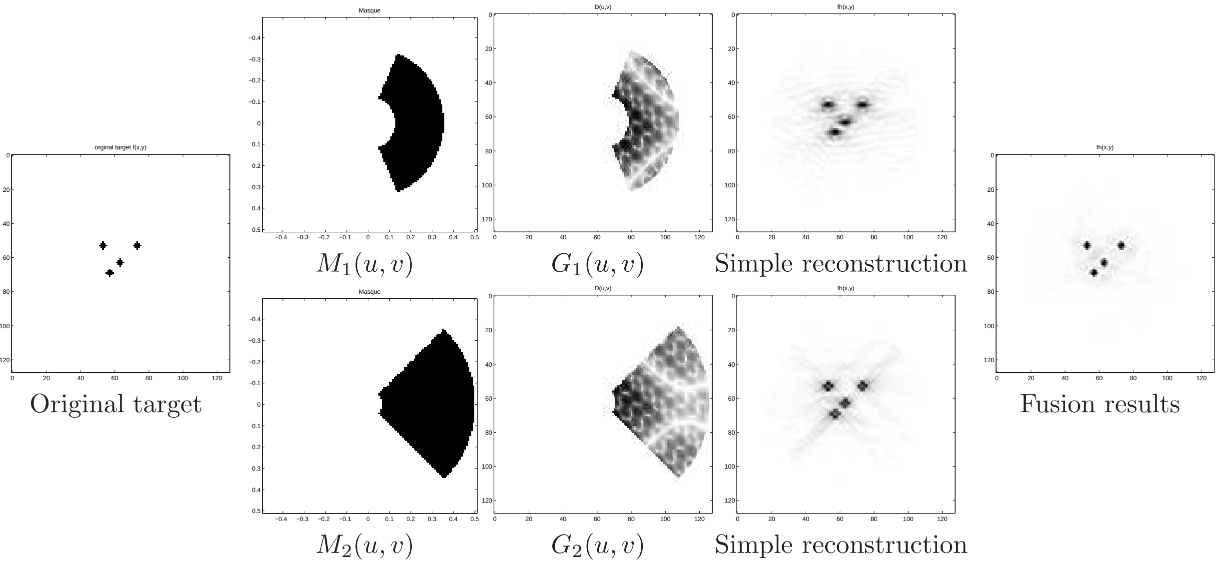

Figure 8. Joint data fusion and inversion on two datasets

6. ACKNOWLEDGEMENTS

The author would like to thank Laboratoire des Signaux et Systèmes in France and Chinese National Key lab: Auto Target Recognition in NUDT. Much appreciation are also given to China Scholarship Council.

REFERENCES

[1] Cheney, M. and Borden, B., "Problems in synthetic-aperture radar imaging," *Inverse problems* **25** (2009).

[2] Idier, J., [*Bayesian Approach to Inverse Problems*], J. Wiley & SonsInc., London, UK (2008).

[3] Hadamard, J., "Sur les problèmes aux derivées patielles et leur signification physique," *Bull. Univ. of Princeton* , 49–52 (1902).

[4] Mohammad-Djafari, A., "Bayesian inference for invese problems in signal and image processing and applications," *International Journal of Imaging Systems and Technology* **16**(5) (2006).

[5] Cheney, M. and Borden, B., [*Fundamentals of Radar Imaging*], SIAM, Philadephia (2009).

[6] Zhu, S. and Mohammad-Djafari, A., "A Bayesian approach to Fourier synthesis inverse problem with application in SAR imaging," in [*30th International Workshop on Bayesian Inference and Mximum Entropy Methods in Science and Engineering*], (4-9 July 2010).

[7] Sulivan, R. J., [*Radar Foundations for Imaging and Advanced Concepts*], Scitech Pub Inc, Raleigh, NC (2004).

[8] Willis, N. J., [*Bistatic-Radar*], Norwood, MA: Artech House (1991).

[9] Gerchberg, R. W., "Superresolution through error energy reduction," *OA* **21**(9), 709–720 (1974).

[10] Adams, M. F. and Anderson, A. P., "Synthetic aperture tomographic (sat) imaging for microwave diagnostics," *Microwaves Optics and Antennas IEE Proceedings H* **129**, 83–88 (1982).

[11] Jones, M. C., "The discrete Gerchberg algorithm," *IEEE ASSP* **34**, 624–626 (1986).

[12] Cetin, M. and Karl, W., "Feature-enhanced synthetic aperture radar image formation based on non-quadratic regularization," *IEEE Trans. Image Processing* **10**, 623–632 (2001).

[13] Mohammad-Djafari, A., "Inverse problems in imaging systems and the general Bayesian inversion frame work," *Journal of Iranian Association of Electrical and Electronics Engineering* **3**(2) (2006).

[14] Mohammad-Djafar, A., Daout, F., and Fargette, P., "Développement de méthodes de fusion et d'inversion de données sar multistatique," in [*GRETSI 2009*], (2009).

[15] Brigham, E., [*The fast Fourier Transform and its application*], Prentice Hall, Englewood Cliffs, NJ (1990).

[16] Chew, W. and Song, J. M., "Fast Fourier transform of sparse spatial data to sparse Fourier data," in [*IEEE Antenna Propag. Int.Symp.*], 2324 – 2327 (2000).

[17] Ding, Y. and Munson, D. C. J., "A fast back-projection algorithm for bistatic SAR imaging," in [*Proc.IEEE Int. Conf.on Image Processing*], 449–452 (2002).

[18] Willis, N. J. and Griffths, H. D., [*Advances in Bistatic radar*], Scitech Pub Inc, Raleigh, NC (2007).

[19] Farina, A. and Grazzini, M., "Radar fusion to detect targets - part ii," *Signal Processing* **82**(8), 1096–1108 (2002).

[20] Mohammd-Djafari, A., "Super-resolution: A short review, a new method based on hidden markov modeling of hr image and future challenges," *the Computer Journal* **52**(1), 126–141 (Mar. 2008).

[21] Zhang, Y., "Understanding image fusion," *Photogrammertic engineering & remote sensing* **70**(6), 657–661 (2004).

[22] Li, Z., *Multi-location Inverse Synthetic Aperture Radar image fusion at the data level*, phd thesis of philosophy, The Pennsylvania State University (Dec. 2007).

[23] Cumming, I. and Wong, F., [*Digital Processing of Synthetic Aperture Radar Data: Algorithms and Implentation*], Aretech House, Norwood MA (2005).

[24] Cetin, M. and Karl, W., "Supersolution and edge-preserving reconstruction of complex-valued synthetic aperture radar images," in [*Proccedings of 2000 IEEE International Conference on Image Processing*], **1**, 701–704 (2000).

[25] Pastina, D., Lombardo, P., Farina, A., and Daddi, P., "Super-resolution of polarimetric SAR images of ship targets," *Siganl Processing* **83**(8), 1737–1748 (2003).

[26] Degraaf, S., "SAR imaging via 2-D spectral estimation methods," *Proc. SPIE on Optical Engineering in Aerospace Sensing* **2230**, 36–49 (1994).

[27] Mohammad-Djafari, A., Zhu, S., Daout, F., and Fargette, P., "Fusion of multistatic synthetic aperture radar data to obtain a superresolution image," in [*2009 Euro American Workshop on Information Optics*], (20-24 July 2009).

[28] Sullvian, J., [*Radar foundation for imaging and advanced concepts*], SciTech Publishing (2004).

[29] Carrara, W., Goodman, R., and Majewski, R., [*Spotlight Synthetic Aperture Radar*], Atrech House, Norwood, MA (1995).

[30] R.Bamler and P.Hartl., "Synthetic aperture radar interferometry," *Inverse Problems* **14**(4), R1–R54 (1998).

[31] Held, D., Brown, W., and Miller, T., "Preliminary results from the NASA/JPL multifrequency, multipolarization SAR," *Proc.1988 IEEE National Radar Conf.*, 7–8 (1988).

[32] Sullivan, R.J., e., "Polarimetric X/L/C-band SAR," *Proc.1998 IEEE National Radar Conf.*, 9–14 (1998).

[33] Tipping, M. E., "Sparse Bayesian learning and the relevance vector machine," *Journal of Machine Learning Research* (2001).